The reversible H + H(-) yields H2(v, j) + e(-) reaction - A consistent description of the associative detachment and dissociative attachment processes using the resonant scattering theory

Jean-Michel Launay, M. Le Dourneuf, C. J. Zeippen

Astron. Astrophys. 252, 842–852 (1991)

ASTRONOMY AND ASTROPHYSICS

The $H+H^- \rightleftharpoons H_2(v, j)+e^-$ reaction: a consistent description of the associative detachment and dissociative attachment processes using the resonant scattering theory

J.M. Launay, M. Le Dourneuf, and C.J. Zeippen

UPR 261 du CNRS et DAMAp, Observatoire de Paris, F-92195 Meudon, France

Received August 11, 1988; accepted April 15, 1991

Abstract. The associative detachment process $H+H^- \rightarrow H_2(v, j) \rightarrow e^-$ and the inverse reaction $H_2(v, j)+e^-$, which leads to rovibrational excitation $[H_2(v', j')+e^-]$ and dissociative attachment $(H+H^-)$, have been calculated consistently using the resonant scattering theory and detailed balance formulae. The evolution of the transient H_2^- molecular complex is governed by a local complex potential, obtained by combining the best short- and long-range potentials available in the literature. The corresponding state-to-state cross-sections for the two reverse reactions agree consistently better with experiment than previous calculations. Cross-sections and reaction rates for many energies in the temperature range of astrophysical interest are presented in tabular and graphical forms.

Key words: H^-, H_2, complex potential – resonant scattering theory – associative detachment – dissociative attachment – electronic collision – rotational excitation – vibrational excitation – interstellar medium – early universe – stellar atmospheres

1. Introduction

The astrophysical importance of the associative detachment (AD) reaction

$$H+H^- \rightarrow H_2(v, j)+e^- \quad (1)$$

has been stressed on a number of occasions. Although grains and three-body reactions produce much more H_2 than the $H+H^-$ atomic reaction, the AD process is efficient under certain conditions as during the recombination epoch. Palla et al. (1983) included the "H^- process" in their study of primordial star formation, and Lepp & Shull (1984) considered the role of the process in the early universe. Moreover, AD populates preferentially highly excited vibration–rotation levels $H_2(v, j)$, which then cascade towards the ground vibrational state by quadrupole radiative transitions, producing a line emission spectrum which is quite different from that resulting from ultraviolet pumping or shock excitation. According to Black et al. (1981), this spectrum is probably too weak to be detected in planetary nebulae, but may be detectable in partly ionized plasmas such as the circumstellar shells of low density. If seen, these lines would provide a means of identifying H_2 in ionized plasmas and of detecting the presence of H^-.

Calculation of the AD spectrum by Black et al. (1981) relies upon the knowledge of cross-sections for populating individual rotation–vibration levels [Eq. (1)]. These have been calculated by Bieniek & Dalgarno (1979, hereafter BD) and Bieniek (1980), using the resonant scattering theory and a semi-empirical complex potential designed to reproduce the only experimental datum available on this reaction, namely the total AD reaction rate measured at 300 K by Schmeltekopf et al. (1967, hereafter SFF) who claim reliability of only a factor of two.

Similar calculations, based also on the resonant scattering theory and including the formation of the same transient complex $H_2^-(^2\Sigma_u)$, have been performed by Wadehra & Bardsley (1978), Bardsley & Wadehra (1979, hereafter BW) and Wadehra (1984) for the reverse process of dissociative attachment (DA):

$$e^- + H_2(v, j) \rightarrow H_2^-(^2\Sigma_u) \rightarrow e^- + H_2(v', j') \quad (2a)$$

$$H_2^-(^2\Sigma_u) \rightarrow H^- + H. \quad (2b)$$

By adjusting the complex potential describing the intermediate resonant state, they obtain results in agreement with several experiments for vibrational excitation [Eq. (2a), measurements by Ehrhardt et al. 1968; Hall 1978] and DA [Eq. (2b), measurements by Schulz & Asundi 1967; Allan & Wong 1978].

In spite of its simplicity and early successes, the resonant scattering theory has been questioned by Nesbet (1981, hereafter N) who pointed out inconsistencies between the actual potentials used to reproduce experimental data on the two reverse processes, Eqs. (1) and (2). The relevance of the resonant scattering theory to H_2^- has been further questioned by Bieniek (1980) and Cederbaum & Domcke (1981), who illustrate limitations of the local potential model, and more recently by Gauyacq (1985, hereafter G) who was able to reproduce the experimental observations without explicit reference to a resonant state in the theory.

However, the resonant scattering theory is still considered, as demonstrated by the recent study of Sakimoto (1989, hereafter S) who, quite independently from the present work, investigated the

Send offprint requests to: C.J. Zeippen

AD process, Eq. (1), using a local complex potential similar, but not identical, to the present one. The aim of S was to examine quantum effects, the zero-energy limit of the cross-section and the validity of the classical orbiting model. He gives rate constants only for four low temperatures in his report.

In this paper, our goal is to show that it is possible to define a single local complex potential to account consistently for all the experimental data concerning the two reverse reactions and to give a large number of partial and total reaction rates which are required in astrophysical applications. A brief summary of the resonant scattering theory is given in Sect. 2: note that the theory has been reviewed by Bardsley (1979) who supplies references to the original work. The potentials selected in the present study are described in Sect. 3. The corresponding cross-sections and reaction rates are compared with previous results in Sect. 4. The main conclusions are summarized in Sect. 5, followed by a brief outline of possible improvements.

2. The resonant scattering theory

A unified treatment of the AD [Eq. (1)] and DA [Eq. (2b)] processes, as well as resonant vibrational excitation [Eq. (2a)] is provided by the resonant scattering theory which, in the case of a broad short-lived resonance, is based on a simple local complex potential (in AU):

$$W(R)=V(R)-\frac{\mathrm{i}}{2}\Gamma(R) \tag{3}$$

which governs the nuclear motion during the lifetime

$$\tau(R)=\frac{\hbar}{\Gamma(R)} \tag{4}$$

of the transient molecular ion, whose energy and width are $V(R)$ and $\Gamma(R)$, respectively. R is the internuclear separation.

More precisely, following BW, the nuclear wavefunction $\xi_j(R)$ describing process (2) satisfies the inhomogeneous complex equation

$$\left[-\frac{1}{2M}\frac{\mathrm{d}^2}{\mathrm{d}R^2}+\frac{j(j+1)}{2MR^2}+W(R)-E\right]\xi_j(R)=\zeta_{vj}(R)\left[\frac{\Gamma(R)}{k(R)}\right]^{1/2} \tag{5}$$

where M is the reduced nuclear mass, j the rotational quantum number, $\zeta_{vj}(R)$ the rovibrational function of the initial $H_2(v, j)$ state, and $k(R)$ the wavenumber of the incident electron which is defined as a function of the potential curves V for H_2^- and V_0 for H_2 by

$$\tfrac{1}{2}k^2(R)=V(R)-V_0(R). \tag{6}$$

The wavefunction describing DA is selected through the regular boundary condition for $R\sim 0$,

$$\xi_j(0)=0 \tag{7a}$$

and the condition of an outgoing spherical wave for $R\to\infty$:

$$\frac{\mathrm{d}\xi_j}{\mathrm{d}R}\to \mathrm{i}K\xi_j \quad \text{with} \quad \frac{K^2}{2M}=E-V(\infty). \tag{7b}$$

It leads to the cross-section for DA (d denotes the dissociated $H+H^-$)

$$\sigma_{vj\to \mathrm{d}}=\frac{\pi K}{MK_{vj}}\lim_{R\to\infty}|\xi_j(R)|^2 \tag{8a}$$

and for resonant vibrational excitation $vj\to v'j$:

$$\sigma_{vj\to v'j}=\frac{\pi k_{v'j}}{k_{vj}}\left[\int \mathrm{d}R\,\zeta_{v'j}(R)\left[\frac{\Gamma(R)}{k(R)}\right]^{1/2}\xi_j(R)\right]^2 \tag{8b}$$

while the cross-section for AD is deduced from Eq. (8a) by the principle of detailed balance:

$$\sigma_{\mathrm{d}\to vj}=(2j+1)g_j\frac{k_{vj}^2}{K^2}\sigma_{vj\to \mathrm{d}}. \tag{8c}$$

Here q_j accounts for the nuclear spin statistics:

$$g_j=\begin{cases}\frac{1}{4} & \text{for even } j\\ \frac{3}{4} & \text{for odd } j.\end{cases} \tag{8d}$$

The preceding formulae neglect the non-local effects associated with the capture and autodetachment of the incident electron [Eq. (6)], as well as the small change ($\Delta j\sim 1$) of the rotational angular momentum due to the electronic capture. Such effects, which have been studied in detail by Bieniek (1980) and Cederbaum & Domcke (1981), mainly affect differential and large j partial cross-sections, but not the bulk of sections needed for astrophysical applications.

Finally, thermal rates are obtained through averaging over a Maxwellian distribution for the initial velocity:

$$\Upsilon_{\mathrm{i}\to\mathrm{f}}(T)=\frac{2}{\sqrt{\pi}v_{\mathrm{i}}}\frac{1}{(kT)^2}\int \mathrm{d}T\,E_{\mathrm{i}}\,\sigma_{\mathrm{i}\to\mathrm{f}}\exp(-E_{\mathrm{i}}/kT). \tag{9}$$

3. Choice of the local complex potential describing the $H_2^-(^2\Sigma_u)$ resonance

The main ingredient of the resonant scattering theory is the local complex potential which controls the nuclear motion [Eq. (5)]. N has pointed out large differences in the real part $V(R)$ of the potentials selected in previous studies which focussed on the compatibility with experiments describing only one of the two reverse processes [Eq. (1) or (2)]. Our aim is mainly to propose a single potential compatible with all known experimental results, and therefore expected to provide reliable partial cross-sections for all transitions.

BD & Bieniek (1980) focussed on AD and obtained a total thermal rate of $1.89\,10^{-9}\,\mathrm{cm^3\,s^{-1}}$, compatible with the experimental datum of SFF ($1.3\,10^{-9}\,\mathrm{cm^3\,s^{-1}}$, reliable to within a factor of 2 according to the authors). This assesses the validity of the long-range part of the BD potential, which accounts properly for the orbiting effects dominating the total cross-section. Hence, in the following, we will use the large-distance part of the BD potential (AU):

$$V_{\mathrm{BD}}(R)=-0.03887R\exp(-0.7441R)-\frac{97}{R^6}-\frac{2.25}{R^4}. \tag{10}$$

In contrast with the total cross-section, partial cross-sections $\sigma_{\mathrm{d}\to vj}$ for the production of excited $H_2(v, j)$ states are sensitive to the internal part of the potential. The disagreement between the BD and BW results for the partial cross-sections for the reverse process [Eq. (2)] combined with the fact that BW have precisely adjusted their potential to reproduce experimental data on resonant vibrational excitation [Eq. (2a), experiments by Ehrhardt et al. 1968; Hall 1978] and DA [Eq. (2b), experiments by Schulz 1959; Rapp et al. 1965] including isotopic effects (Schulz &

Asundi 1967; Allan & Wong 1978), lead us to prefer the BW short-range complex potential, i.e.

$$V_{BW}(R)=V_0(R)-A+0.2152\exp(-0.2276R^2) \quad (11a)$$

$$\Gamma_{BW}(R)=Ck^3(R) \quad (11b)$$

where A is the affinity of H^- (0.02271 AU) and C a constant chosen either to optimize the agreement with experiment for the isotopic effect H_2/D_2 or the near-threshold DA cross-section for H_2:

$$C=2.65 \text{ AU} \quad \text{or} \quad C=2.966 \text{ AU} \quad (11c)$$

In the following, we have adopted $C=2.65$ AU, which consistently leads to better isotopic effects and H_2 threshold DA cross-section when used in addition to the V_{BD} long-range potential [Eq. (10)].

In order to test the sensitivity of the results to the potential used, we have performed two series of calculations based on the same potentials at short range, i.e.

$$V^{(1)}_{SR}(R)=V^{(2)}_{SR}(R)=V_{BW}(R), \quad \text{as in Eq. (11) for } R\leq 3a_0 \quad (12)$$

and long range,

$$V^{(1)}_{LR}(R)=V^{(2)}_{LR}(R)=V_{BD}(R), \quad \text{as in Eq. (10) for large } R \quad (13)$$

while in the middle range, we have tested either a simple interpolation function

$$V^{(1)}_{MR}(R)=a^{(1)}+\frac{b^{(1)}}{R^2}+\frac{c^{(1)}}{R^4}+\frac{d^{(1)}}{R^6} \quad \text{for} \quad 3a_0\leq R\leq 6.5a_0 \quad (14a)$$

with

$$a^{(1)}=-1.02098, \quad b^{(1)}=-0.52349,$$
$$c^{(1)}=3.25035, \quad d^{(1)}=-12.97693 \quad (14b)$$

or the results of a recent *ab initio* calculation based on a multi-reference configuration interaction approach (Senekowitsch et al. 1984, hereafter SRDW), combined with a matching interpolation function

$$V^{(2)}_{MR}(R)=\begin{cases} V_{SRDW}(R), & \text{for } 3a_0\leq R\leq 10a_0 \\ a^{(2)}+\dfrac{b^{(2)}}{R^2}+\dfrac{c^{(2)}}{R^4}+\dfrac{d^{(2)}}{R^6}, & \text{for } 10a_0\leq R\leq 20a_0 \end{cases} \quad (15a)$$

with

$$a^{(2)}=-1.02792, \quad b^{(2)}=0.61132,$$
$$c^{(2)}=-142.24904, \quad d^{(2)}=5922.30460. \quad (15b)$$

The difference between the two potentials, later on referred to as $V^{(1)}$ and $V^{(2)}$, is summarized in Table 1 and illustrated in Fig. 1. Note that the SRDW potential has been slightly adjusted so as to ensure proper matching with the BW potential at $R=3a_0$.

It should be noted here that S also used the short-range potential proposed by BW [Eqs. (11)] up to $R=3a_0$ and the middle-range potential calculated by SRDW up to $R=6a_0$. The difference between his potential and the present $V^{(2)}$ form concerns the range above $6a_0$: we include the SRDW values up to $R=10a_0$, we keep the long-range potential proposed by BD for large R and we connect those two potentials with a fitting formula in the range $10a_0\leq R\leq 20a_0$ [see Eqs. (15)], while S uses his own fitting formula throughout. The importance of this difference between the two potentials will become apparent in Sect. 4.

Table 1. Middle-range potentials for $H+H(^1\Sigma_g^+)$, $V_0(R)$, and for $H+H^-(^2\Sigma_u^+)$, $V^{(1)}(R)$ and $V^{(2)}(R)$, used in the present work (see text). All values in AU

R	V_0	$V^{(1)}$	$V^{(2)}$
3.0	−1.056852	−1.056821	−1.056821
3.25	−1.042716	−1.052421	−1.053631
3.5	−1.031361	−1.049115	−1.051821
4.0	−1.015876	−1.044171	−1.048227
5.0	−1.003258	−1.037551	−1.042543
6.0	−1.000305	−1.033293	−1.038162
8.0	−0.999524	−1.028900	−1.032776
10.0	−0.999477	−1.027722	−1.030109
15.0	−0.999469	−1.027234	−1.027493
20.0	−0.999456	−1.027188	−1.027188

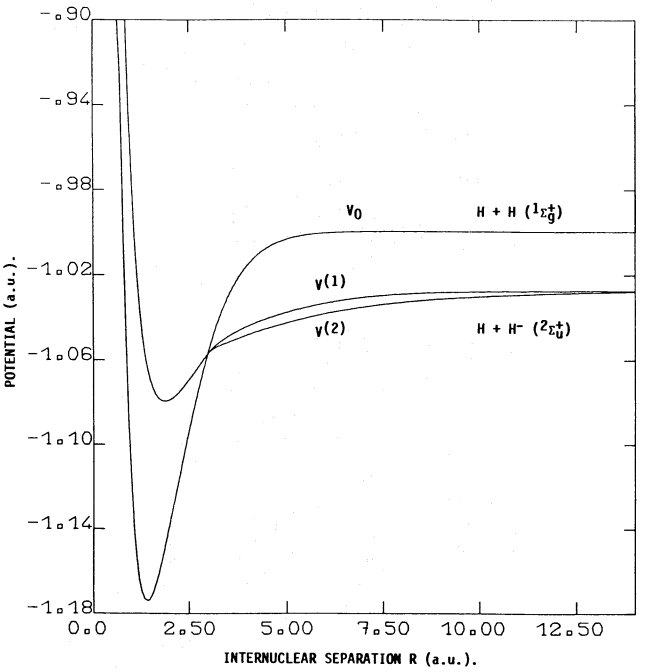

Fig. 1. Potentials used in the present work. V_0 is from Bishop & Shih (1976) while $V^{(1)}$ and $V^{(2)}$ are combinations of various functions (see text). Note that $V^{(2)}$, the preferred potential, is considerably more attractive in the middle range than $V^{(1)}$

The choice of the H_2 potential $V_0(R)$ is much simpler, since very accurate potentials have been proposed by Kolos & Wolniewicz (1965, 1966, 1968) and Bishop & Shih (1976). The choice of one or the other hardly affects the present calculation, so that all the calculations discussed below were performed with the latter.

4. Results

The problem was solved numerically using a set of programs based on the de Vogelaere integration algorithm. Cross-sections

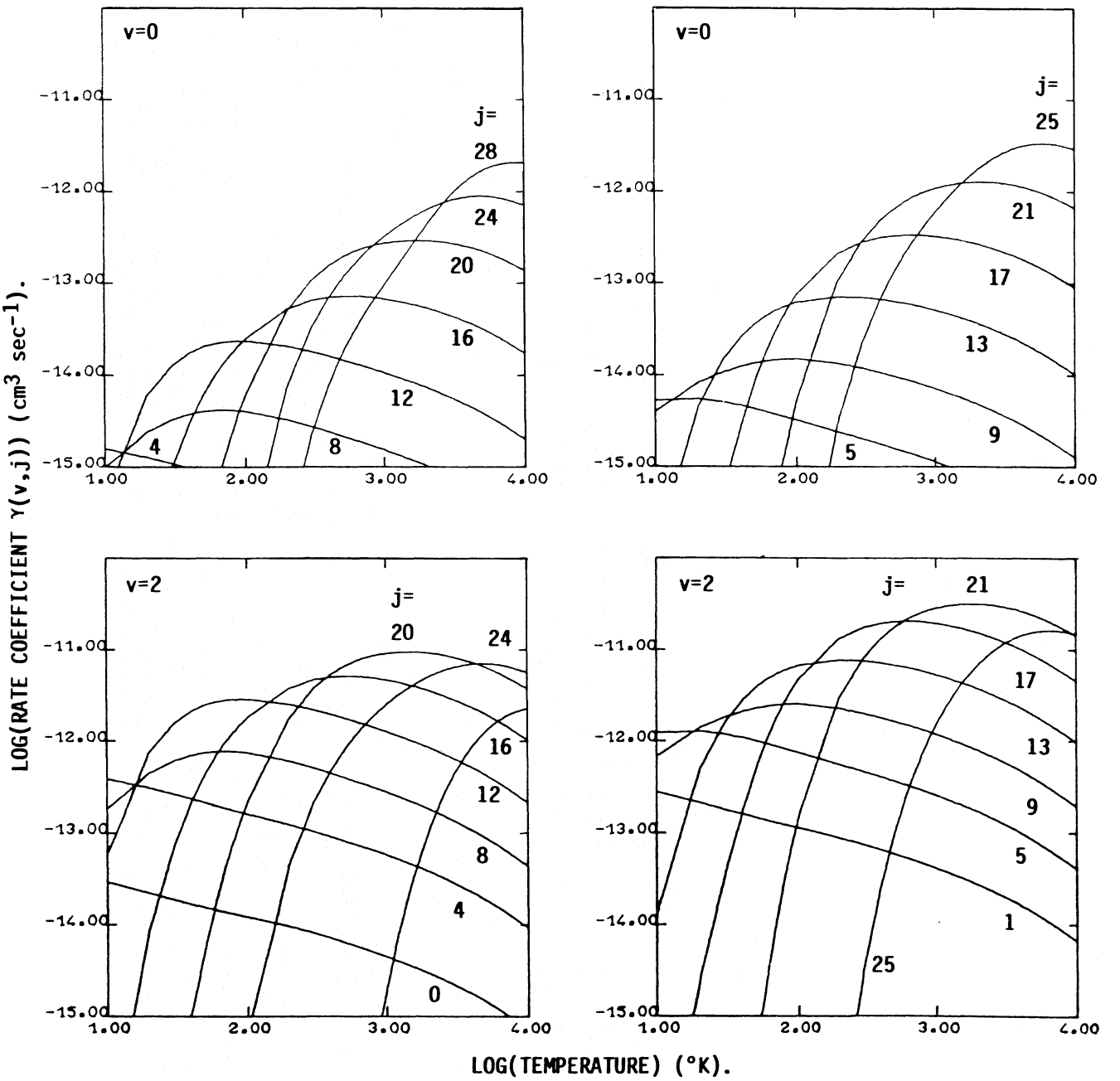

Fig. 2a

Fig. 2a–c. Variation with temperature of present selected individual rate coefficients $\Upsilon(v, j)$ obtained with potential $V^{(2)}$

for AD in which H_2 is left in a specific rovibrational level (v, j) were calculated, in particular, for relative energies of 0.0129, 0.129 and 0.646 eV, chosen by BD & Bieniek (1980). Results for those and other relative energies may be obtained on request from the authors. Broadly speaking., when considering the results obtained with potential $V^{(1)}$, it appears that the characteristics of the present cross-sections are similar to those published previously, but there are discrepancies for individual cross-sections which can be of the order of a factor of 2. Therefore, the branching ratios would be affected. Inspecting the results obtained with potential $V^{(2)}$, it turns out that the individual cross-sections are generally smaller than the ones obtained with $V^{(1)}$, but for higher js the gap decreases and is even inverted for very large j. As shown below, potential $V^{(2)}$ marks a real improvement over other potentials like $V^{(1)}$. Therefore, we present in Table 2 rate coefficients for populating the rovibrational levels (v, j) of H_2 by AD, and obtained with the complex potential $V^{(2)}$. Figure 2 shows the variation with temperature of the individual rate coefficients $\Upsilon(v, j)$.

The total cross-sections obtained with $V^{(1)}$ come close to the ones of BD & Bieniek (1980): the present $V^{(1)}$ thermal rate coefficient at 300 K is found to be $2.03\ 10^{-9}\,cm^3\,s^{-1}$, as compared to the previous value of $1.89\ 10^{-9}\,cm^3\,s^{-1}$ (the disagreement is less than 7.5%). When using $V^{(2)}$, the thermal rate

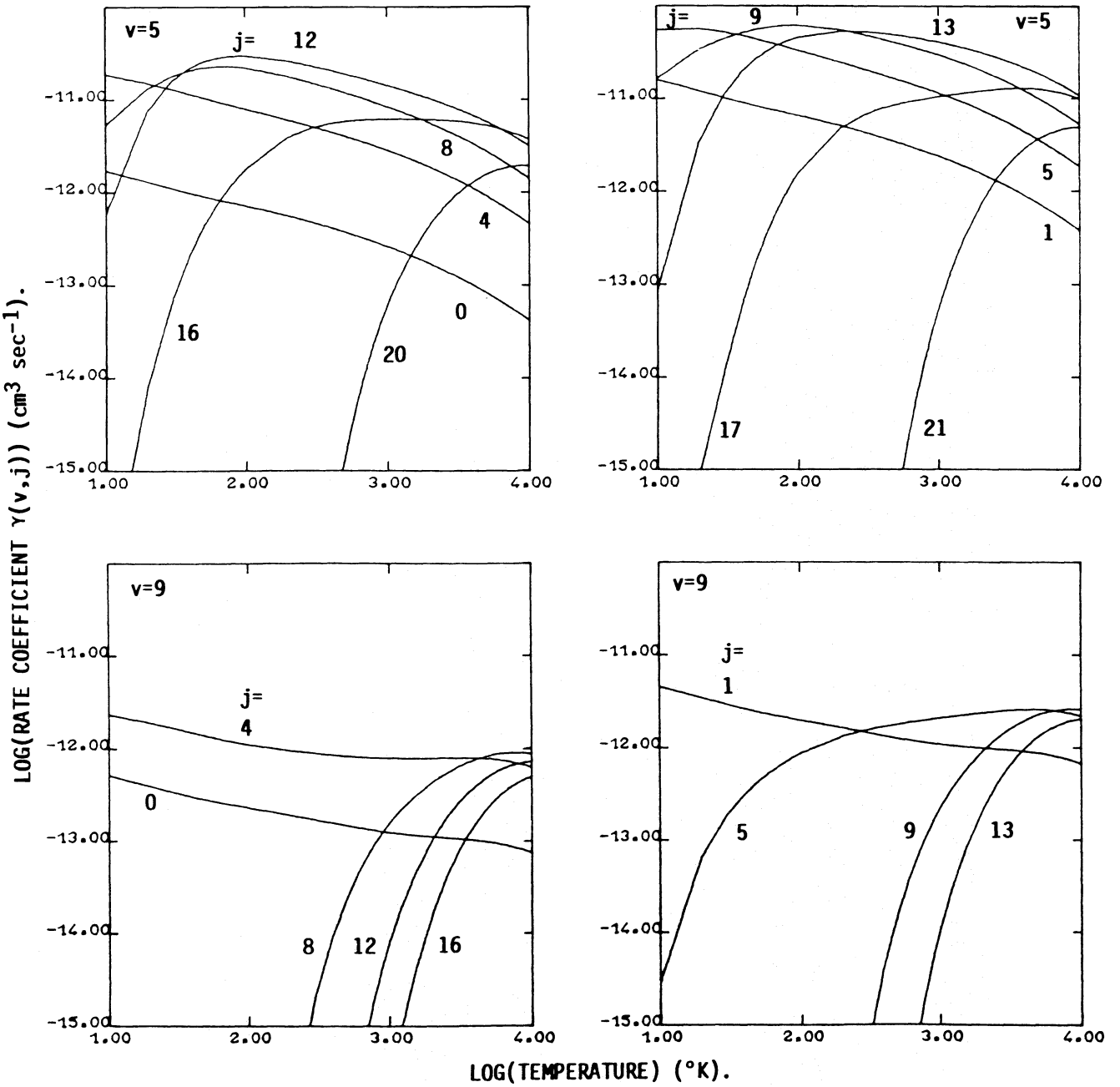

Fig. 2b

coefficient at 300 K turns out to be $1.49\,10^{-9}\,cm^3\,s^{-1}$, i.e. over 20% less than the value obtained with $V^{(1)}$, and only about 15% above the experimental value of SFF. This seems to indicate that the SRDW potential is indeed more accurate than previous ones, as claimed by the authors. However, one must bear in mind that the uncertainty in the measured value for the thermal rate coefficient is a factor of 2. Figure 3 displays the variation with temperature of the thermal rate coefficients obtained with $V^{(1)}$ and $V^{(2)}$.

Turning now to the study of S, one notes that for a relative energy of 0.0129 eV, he reports a total AD cross-section of 772 AU, as compared to the value of 321 AU calculated by Bieniek (1980), i.e. more than a factor of 2 higher. Let us recall at this point that the present total cross-sections obtained with $V^{(1)}$ are similar to the findings of BD & Bieniek (1980) while there is a decrease when $V^{(2)}$ is used. Of course, this shows up when comparing the AD rate constant calculated by S at 10 K with the present one obtained with $V^{(2)}$: 2.77 and $1.09\,10^{-9}\,cm^3\,s^{-1}$, respectively. The discrepancy between the two results is nearly a factor of 3. Now, S states that his rate of $5\,10^{-9}\,cm^3\,s^{-1}$ at a relative energy close to 0.01 eV is larger than data extrapolated from experimental work. Even taking the factor of 2 uncertainty on the thermal rate measured by SFF into account, it would appear that the rates calculated by S could be out of the error

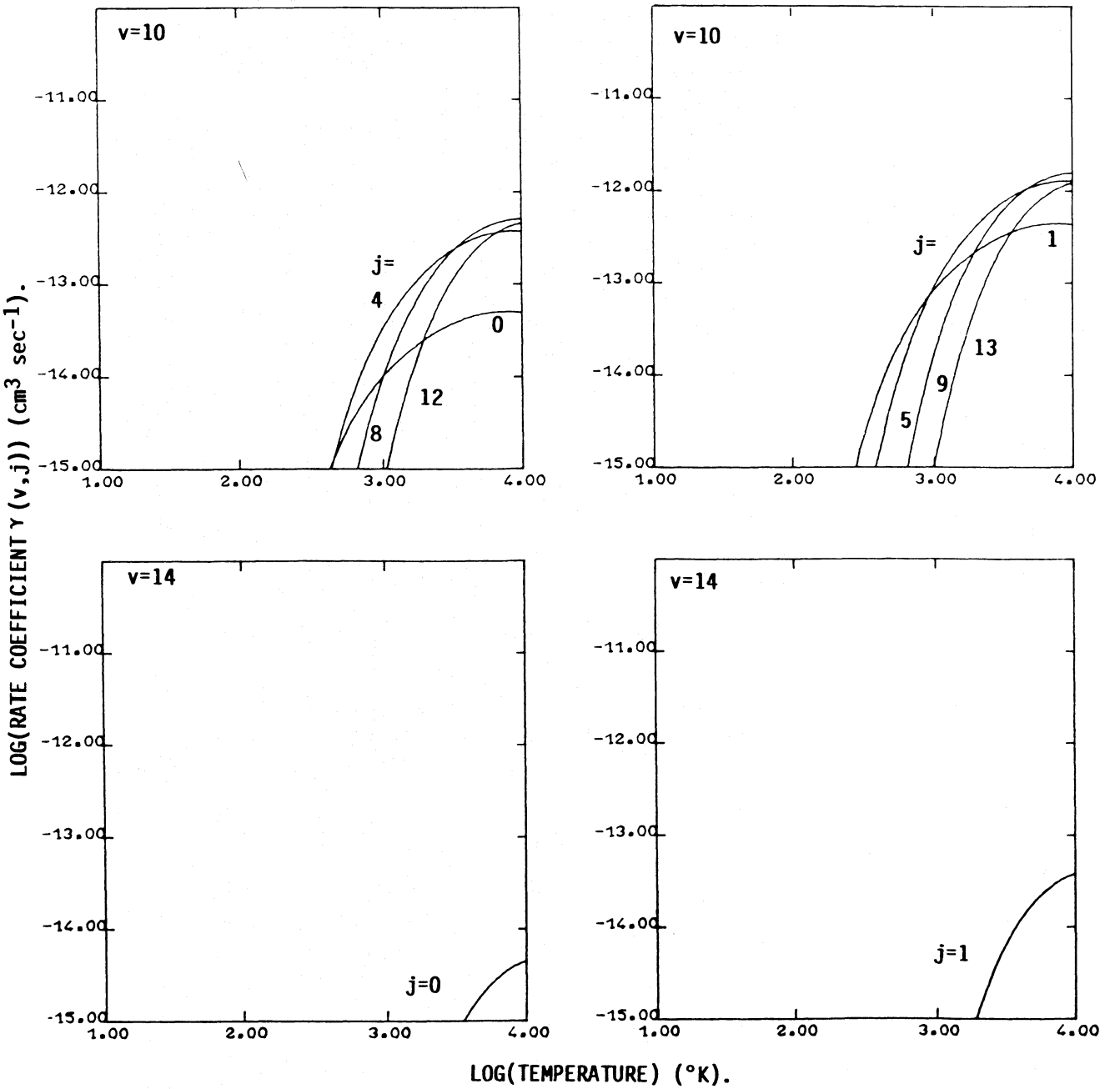

Fig. 2c

bars by as much as a factor of 2. This indicates that the long-range potential adopted by this author is not reliable. It must be agreed that his suggestion to perform accurate measurements at low energies in order to provide more checks on the long-range potential is well justified.

Considering now the DA process, a comparison is made in Table 3 between the near-threshold cross-sections by BW and the present results obtained with potentials $V^{(1)}$ and $V^{(2)}$. It is seen that the $V^{(1)}$ values are close to the BW results for $j=0$ and $v\geq 3$, while the $V^{(2)}$ values are close to the BW results for $j\leq 5$ and $v\leq 2$. Most results are within a factor of 2.

It is remarkable that the $V^{(1)}$ cross section at threshold is close to the value obtained by Wadehra & Bardsley (1978) who used $C=2.65$ AU, unlike BW who used $C=2.966$ AU. In the present calculations, we chose the lower value for C [Eq. (11c)] because with $V^{(2)}$ it yields a ratio of 377 between the near-threshold DA cross-sections for H_2 and D_2, which is slightly better than the value of BW (410) with the same C. As the inclusion of $V^{(2)}$ in our calculation allows for a decrease of the near-threshold DA H_2 cross-section down to the BW (and the experimental) findings, we favoured the lower C.

Recently, G used an effective-range approximation to treat the DA process. He does not introduce a resonant H_2^- state as an intermediate state in the process, but he assumes that the electron is captured directly via a non-adiabatic coupling into a negative-energy state. His results are compared with ours in Table 4. The

Table 2. Individual rate coefficients for populating the rovibrational levels $H_2(v, j)$ of energies ε_{vj} in K, with the energy of $H + H^-$ at an infinite distance as origin) by associative detachment of H and H^-, tabulated as $-\log \Upsilon(v, j)$ (in $cm^3\ s^{-1}$)

v	j	ε_{vj}	10K	30K	100K	300K	1000K	3000K	10^4K	j	ε_{vj}	10K	30K	100K	300K	1000K	3000K	10^4K
0	0	−43218.	15.97	16.16	16.35	16.52	16.78	17.08	17.56	1	−43047.	14.98	15.18	15.37	15.55	15.80	16.11	16.58
	2	−42708.	15.17	15.38	15.58	15.76	16.02	16.32	16.79	3	−42202.	14.45	14.67	14.89	15.08	15.33	15.63	16.11
	4	−41536.	14.80	14.96	15.18	15.37	15.62	15.92	16.39	5	−40713.	14.27	14.29	14.49	14.69	14.95	15.25	15.72
	6	−39743.	14.62	14.51	14.71	14.95	15.22	15.52	16.00	7	−38631.	14.27	13.95	14.04	14.26	14.54	14.84	15.32
	8	−37387.	15.01	14.48	14.39	14.56	14.81	15.12	15.59	9	−36020.	14.40	13.97	13.82	13.92	14.14	14.43	14.90
	10	−34540.	15.12	14.36	14.18	14.23	14.42	14.70	15.16	11	−32955.	14.68	13.65	13.49	13.55	13.74	14.01	14.46
	12	−31277.	15.33	13.90	13.63	13.75	13.97	14.25	14.70	13	−29514.	15.92	13.83	13.21	13.16	13.29	13.55	13.99
	14	−27676.	17.41	14.73	13.68	13.48	13.55	13.78	14.22	15	−25773.	16.95	14.62	13.30	12.88	12.88	13.09	13.51
	16	−23813.	18.31	15.01	13.60	13.19	13.17	13.36	13.77	17	−21804.	19.03	15.24	13.13	12.55	12.48	12.65	13.05
	18	−19756.	20.28	16.48	13.75	12.90	12.74	12.88	13.27	19	−17676.	19.42	15.73	13.59	12.46	12.17	12.25	12.59
	20	−15572.	21.38	17.48	14.22	12.97	12.56	12.56	12.86	21	−13449.	23.72	19.23	14.28	12.54	11.96	11.90	12.18
	22	−11316.	25.11	19.43	15.31	13.18	12.45	12.27	12.48	23	−9178.	27.64	21.17	15.46	12.87	11.99	11.70	11.84
	24	−7041.	30.97	23.64	15.92	13.49	12.50	12.08	12.15	25	−4911.	31.25	24.26	16.92	13.65	12.22	11.58	11.53
	26	−2793.	36.14	25.61	18.05	14.35	12.79	12.02	11.89	27	−692.	39.26	28.34	17.71	14.01	12.41	11.53	11.30
	28	1386.	12.35	12.55	12.67	12.63	12.43	11.82	11.62									
1	0	−37229.	14.56	14.75	14.94	15.12	15.38	15.69	16.17	1	−37067.	13.58	13.78	13.97	14.15	14.40	14.71	15.20
	2	−36745.	13.77	13.98	14.19	14.37	14.62	14.93	15.41	3	−36265.	13.06	13.28	13.50	13.69	13.94	14.25	14.73
	4	−35632.	13.42	13.58	13.80	13.99	14.24	14.55	15.03	5	−34851.	12.90	12.92	13.12	13.33	13.58	13.89	14.37
	6	−33930.	13.26	13.16	13.36	13.60	13.87	14.18	14.66	7	−32875.	12.92	12.61	12.70	12.92	13.20	13.51	14.00
	8	−31695.	13.68	13.15	13.07	13.24	13.50	13.80	14.29	9	−30398.	13.09	12.66	12.52	12.62	12.85	13.14	13.62
	10	−28995.	13.83	13.08	12.89	12.94	13.15	13.43	13.91	11	−27494.	13.42	12.39	12.22	12.28	12.48	12.77	13.23
	12	−25905.	14.09	12.66	12.39	12.51	12.74	13.03	13.50	13	−24236.	14.70	12.61	11.99	11.94	12.09	12.35	12.81
	14	−22498.	16.22	13.54	12.49	12.29	12.37	12.62	13.07	15	−20699.	15.78	13.45	12.13	11.72	11.73	11.95	12.40
	16	−18847.	17.17	13.86	12.47	12.05	12.05	12.25	12.68	17	−16952.	17.92	14.13	12.02	11.44	11.39	11.58	12.00
	18	−15021.	19.19	15.40	12.66	11.82	11.67	11.84	12.25	19	−13061.	18.36	14.67	12.53	11.41	11.14	11.24	11.61
	20	−11081.	20.35	16.45	13.20	11.95	11.56	11.60	11.93	21	−9086.	22.73	18.23	13.30	11.56	10.99	10.98	11.29
	22	−7084.	24.15	18.47	14.37	12.25	11.53	11.39	11.65	23	−5081.	26.74	20.27	14.57	11.98	11.12	10.88	11.06
	24	−3082.	30.14	22.81	15.10	12.66	11.69	11.33	11.44	25	−1095.	30.58	23.58	16.20	12.91	11.50	10.90	10.90
	26	876.	17.19	16.67	13.66	12.50	11.80	11.31	11.30	27	2825.	10.60	10.82	11.01	11.10	10.98	10.67	10.73
	28	4746.	11.44	11.60	11.67	11.58	11.32	11.04	11.14									
2	0	−31580.	13.53	13.72	13.91	14.09	14.35	14.67	15.15	1	−31426.	12.55	12.75	12.94	13.12	13.38	13.70	14.18
	2	−31120.	12.75	12.96	13.17	13.35	13.61	13.92	14.40	3	−30665.	12.04	12.26	12.49	12.68	12.93	13.25	13.73
	4	−30065.	12.41	12.58	12.79	12.98	13.24	13.55	14.04	5	−29325.	11.91	11.93	12.13	12.33	12.59	12.90	13.39
	6	−28451.	12.28	12.18	12.38	12.62	12.89	13.21	13.70	7	−27452.	11.96	11.65	11.73	11.96	12.24	12.56	13.05
	8	−26335.	12.74	12.21	12.12	12.30	12.56	12.87	13.36	9	−25108.	12.17	11.74	11.60	11.70	11.93	12.23	12.72
	10	−23781.	12.93	12.18	11.99	12.04	12.25	12.55	13.02	11	−22361.	12.54	11.51	11.35	11.41	11.61	11.90	12.38
	12	−20860.	13.24	11.81	11.54	11.66	11.90	12.20	12.67	13	−19285.	13.88	11.79	11.17	11.12	11.27	11.55	12.01
	14	−17645.	15.43	12.74	11.70	11.50	11.59	11.84	12.31	15	−15949.	15.02	12.69	11.37	10.96	10.98	11.21	11.67
	16	−14205.	16.44	13.14	11.74	11.33	11.33	11.55	11.99	17	−12423.	17.23	13.44	11.33	10.76	10.71	10.91	11.34
	18	−10608.	18.55	14.75	12.02	11.18	11.04	11.22	11.65	19	−8770.	17.77	14.07	11.94	10.82	10.56	10.67	11.06
	20	−6915.	19.81	15.92	12.66	11.42	11.04	11.09	11.43	21	−5050.	22.26	17.77	12.83	11.09	10.54	10.53	10.85
	22	−3181.	23.77	18.10	13.99	11.87	11.16	11.03	11.28	23	−1317.	26.51	20.04	14.31	11.72	10.86	10.61	10.78
	24	538.	17.21	15.69	12.84	11.89	11.37	11.11	11.23	25	2377.	11.14	11.26	11.24	11.07	10.78	10.58	10.73
	26	4192.	10.64	10.86	11.07	11.19	11.16	11.06	11.21	27	5978.	10.61	10.80	10.93	10.91	10.76	10.65	10.78
	28	7727.	10.81	11.03	11.25	11.38	11.34	11.22	11.31									
3	0	−26262.	12.76	12.95	13.14	13.32	13.58	13.90	14.38	1	−26116.	11.78	11.98	12.17	12.35	12.61	12.93	13.41
	2	−25827.	11.99	12.19	12.40	12.58	12.84	13.16	13.64	3	−25396.	11.28	11.50	11.73	11.92	12.18	12.49	12.98
	4	−24828.	11.66	11.83	12.04	12.24	12.49	12.81	13.29	5	−24128.	11.17	11.19	11.39	11.60	11.86	12.17	12.66
	6	−23302.	11.56	11.46	11.66	11.90	12.18	12.50	12.98	7	−22358.	11.26	10.94	11.03	11.26	11.54	11.87	12.36
	8	−21303.	12.05	11.53	11.44	11.61	11.88	12.19	12.68	9	−20145.	11.50	11.08	10.93	11.04	11.27	11.58	12.06
	10	−18892.	12.30	11.54	11.35	11.41	11.62	11.92	12.40	11	−17555.	11.93	10.90	10.74	10.80	11.01	11.30	11.77
	12	−16140.	12.66	11.22	10.96	11.08	11.32	11.62	12.10	13	−14658.	13.33	11.24	10.62	10.58	10.73	11.01	11.47
	14	−13116.	14.92	12.23	11.19	10.99	11.08	11.34	11.80	15	−11524.	14.56	12.23	10.91	10.50	10.52	10.75	11.20
	16	−9889.	16.03	12.73	11.33	10.92	10.92	11.14	11.57	17	−8220.	16.89	13.10	10.99	10.42	10.37	10.56	10.97
	18	−6524.	18.29	14.49	11.76	10.92	10.77	10.93	11.34	19	−4809.	17.61	13.91	11.78	10.66	10.38	10.47	10.81
	20	−3083.	19.78	15.88	12.62	11.38	10.98	10.98	11.26	21	−1351.	22.41	17.91	12.96	11.21	10.63	10.56	10.78
	22	377.	15.38	15.32	12.83	11.74	11.31	11.16	11.30	23	2097.	10.39	10.61	10.83	10.92	10.83	10.72	10.84
	24	3799.	11.09	11.29	11.47	11.50	11.39	11.26	11.34	25	5477.	10.59	10.82	11.04	11.14	11.04	10.86	10.91
	26	7123.	11.53	11.72	11.84	11.81	11.61	11.40	11.43	27	8726.	10.50	10.72	10.93	11.05	11.03	10.92	10.98

Table 2 (continued)

v	j	ϵ_{vj}	10K	30K	100K	300K	1000K	3000K	10^4K	j	ϵ_{vj}	10K	30K	100K	300K	1000K	3000K	10^4K
4	0	−21271.	12.18	12.37	12.56	12.74	13.01	13.32	13.81	1	−21134.	11.21	11.41	11.60	11.78	12.04	12.36	12.84
	2	−20860.	11.42	11.63	11.83	12.02	12.28	12.59	13.08	3	−20454.	10.73	10.94	11.17	11.36	11.62	11.94	12.42
	4	−19918.	11.12	11.28	11.49	11.69	11.94	12.26	12.74	5	−19258.	10.63	10.66	10.85	11.06	11.32	11.64	12.12
	6	−18480.	11.04	10.94	11.13	11.38	11.66	11.98	12.46	7	−17590.	10.75	10.44	10.53	10.76	11.04	11.36	11.85
	8	−16596.	11.57	11.04	10.96	11.13	11.39	11.71	12.20	9	−15507.	11.05	10.62	10.48	10.58	10.81	11.12	11.60
	10	−14330.	11.87	11.11	10.92	10.98	11.19	11.48	11.96	11	−13074.	11.54	10.51	10.34	10.41	10.61	10.89	11.36
	12	−11747.	12.31	10.87	10.61	10.73	10.96	11.25	11.72	13	−10359.	13.03	10.95	10.33	10.27	10.42	10.68	11.13
	14	−8917.	14.69	12.00	10.96	10.76	10.83	11.06	11.50	15	−7430.	14.41	12.08	10.76	10.34	10.34	10.54	10.95
	16	−5906.	15.99	12.68	11.28	10.86	10.84	11.00	11.37	17	−4353.	16.97	13.18	11.06	10.48	10.40	10.52	10.85
	18	−2779.	18.54	14.74	12.00	11.15	10.96	11.03	11.31	19	−1192.	18.12	14.42	12.25	11.10	10.76	10.70	10.87
	20	400.	12.06	12.18	12.06	11.70	11.49	11.33	11.40	21	1990.	10.60	10.82	11.03	11.12	11.05	10.90	10.95
	22	3570.	11.74	11.89	11.94	11.83	11.62	11.43	11.47	23	5132.	10.62	10.84	11.04	11.13	11.09	10.97	11.02
	24	6667.	10.92	11.15	11.37	11.50	11.51	11.44	11.51	25	8164.	11.50	11.59	11.55	11.38	11.14	10.99	11.05
5	0	−16606.	11.76	11.96	12.15	12.33	12.59	12.90	13.38	1	−16477.	10.80	10.99	11.18	11.37	11.62	11.94	12.42
	2	−16220.	11.01	11.22	11.42	11.61	11.86	12.18	12.66	3	−15838.	10.32	10.54	10.77	10.96	11.21	11.53	12.01
	4	−15334.	10.73	10.89	11.10	11.30	11.55	11.86	12.34	5	−14714.	10.26	10.28	10.48	10.69	10.94	11.25	11.73
	6	−13984.	10.69	10.58	10.78	11.02	11.29	11.60	12.09	7	−13149.	10.42	10.11	10.20	10.42	10.70	11.01	11.49
	8	−12218.	11.27	10.74	10.66	10.83	11.08	11.38	11.86	9	−11198.	10.78	10.36	10.21	10.31	10.53	10.81	11.28
	10	−10097.	11.65	10.90	10.71	10.76	10.95	11.22	11.66	11	−8923.	11.38	10.36	10.19	10.24	10.43	10.67	11.10
	12	−7686.	12.23	10.80	10.53	10.64	10.85	11.09	11.50	13	−6393.	13.05	10.97	10.34	10.28	10.39	10.59	10.96
	14	−5053.	14.83	12.14	11.09	10.87	10.91	11.06	11.40	15	−3675.	14.70	12.36	11.03	10.60	10.55	10.64	10.93
	16	−2266.	16.47	13.16	11.75	11.30	11.21	11.23	11.43	17	−834.	17.75	13.95	11.80	11.18	10.98	10.89	11.00
	18	611.	11.70	11.76	11.76	11.72	11.61	11.48	11.52	19	2062.	10.64	10.87	11.08	11.20	11.17	11.03	11.06
	20	3510.	12.15	12.21	12.11	11.90	11.67	11.52	11.56	21	4947.	10.73	10.94	11.11	11.15	11.10	11.02	11.09
	22	6362.	10.98	11.20	11.40	11.52	11.53	11.48	11.57	23	7746.	10.46	10.69	10.91	11.05	11.07	11.01	11.09
6	0	−12270.	11.50	11.70	11.88	12.06	12.31	12.60	13.07	1	−12149.	10.54	10.73	10.93	11.10	11.35	11.64	12.11
	2	−11908.	10.76	10.97	11.17	11.35	11.59	11.88	12.35	3	−11550.	10.09	10.31	10.53	10.72	10.96	11.25	11.71
	4	−11079.	10.52	10.68	10.89	11.08	11.31	11.59	12.05	5	−10500.	10.08	10.10	10.29	10.49	10.73	11.01	11.46
	6	−9818.	10.54	10.43	10.63	10.86	11.11	11.39	11.83	7	−9039.	10.32	10.01	10.09	10.31	10.56	10.83	11.26
	8	−8172.	11.23	10.70	10.61	10.77	11.00	11.25	11.66	9	−7222.	10.81	10.38	10.23	10.32	10.51	10.73	11.12
	10	−6200.	11.77	11.01	10.81	10.85	11.01	11.20	11.56	11	−5112.	11.60	10.57	10.40	10.44	10.58	10.74	11.05
	12	−3967.	12.57	11.14	10.86	10.96	11.12	11.25	11.52	13	−2773.	13.54	11.45	10.82	10.73	10.78	10.85	11.06
	14	−1540.	15.48	12.79	11.72	11.48	11.43	11.43	11.57	15	−275.	15.67	13.29	11.89	11.39	11.20	11.09	11.15
	16	1012.	11.64	11.78	11.84	11.85	11.74	11.61	11.64	17	2313.	11.24	11.42	11.50	11.40	11.23	11.11	11.16
	18	3620.	11.55	11.73	11.83	11.77	11.64	11.55	11.63	19	4921.	10.77	10.98	11.14	11.18	11.12	11.05	11.14
	20	6209.	11.13	11.35	11.54	11.62	11.60	11.53	11.61	21	7471.	10.65	10.87	11.07	11.18	11.18	11.10	11.16
	22	8693.	11.22	11.44	11.65	11.76	11.74	11.64	11.68									
7	0	−8266.	11.51	11.70	11.89	12.05	12.27	12.50	12.90	1	−8154.	10.56	10.75	10.94	11.10	11.32	11.55	11.94
	2	−7930.	10.80	11.00	11.20	11.37	11.58	11.81	12.19	3	−7598.	10.15	10.37	10.59	10.76	10.97	11.19	11.57
	4	−7160.	10.61	10.77	10.98	11.16	11.36	11.57	11.94	5	−6623.	10.22	10.24	10.43	10.62	10.82	11.02	11.37
	6	−5990.	10.74	10.64	10.83	11.05	11.26	11.45	11.78	7	−5270.	10.59	10.28	10.36	10.57	10.78	10.95	11.26
	8	−4468.	11.58	11.05	10.95	11.10	11.28	11.44	11.71	9	−3593.	11.25	10.82	10.66	10.74	10.87	10.99	11.22
	10	−2652.	12.29	11.53	11.32	11.34	11.44	11.52	11.70	11	−1653.	12.19	11.16	10.98	11.00	11.07	11.10	11.24
	12	−606.	13.28	11.84	11.55	11.60	11.66	11.64	11.73	13	482.	11.41	11.40	11.36	11.33	11.27	11.20	11.26
	14	1601.	11.29	11.51	11.69	11.74	11.71	11.64	11.72	15	2743.	10.77	10.99	11.17	11.24	11.21	11.14	11.22
	16	3898.	11.24	11.45	11.64	11.72	11.69	11.61	11.69	17	5056.	10.78	11.00	11.19	11.27	11.24	11.15	11.21
	18	6206.	11.30	11.51	11.71	11.79	11.76	11.66	11.71	19	7338.	10.86	11.07	11.26	11.33	11.31	11.22	11.26
	20	8436.	11.49	11.70	11.87	11.93	11.83	11.72	11.77									
8	0	−4607.	11.89	12.08	12.25	12.41	12.59	12.73	12.98	1	−4503.	10.94	11.13	11.31	11.47	11.64	11.78	12.03
	2	−4297.	11.19	11.40	11.59	11.75	11.92	12.05	12.29	3	−3991.	10.57	10.78	11.00	11.16	11.33	11.45	11.68
	4	−3589.	11.05	11.21	11.41	11.57	11.74	11.85	12.07	5	−3095.	10.67	10.69	10.88	11.06	11.22	11.33	11.53
	6	−2515.	11.21	11.10	11.29	11.50	11.67	11.77	11.96	7	−1856.	11.07	10.76	10.83	11.02	11.19	11.28	11.44
	8	−1123.	12.08	11.55	11.45	11.57	11.70	11.75	11.90	9	−326.	11.91	11.46	11.27	11.29	11.31	11.30	11.40
	10	528.	11.74	11.85	11.87	11.87	11.84	11.78	11.85	11	1430.	11.17	11.37	11.51	11.50	11.37	11.27	11.34
	12	2373.	12.18	12.29	12.26	12.08	11.86	11.74	11.80	13	3346.	10.87	11.09	11.31	11.40	11.35	11.25	11.31
	14	4340.	11.26	11.49	11.71	11.84	11.83	11.74	11.79	15	5344.	10.79	11.01	11.22	11.35	11.36	11.29	11.33
	16	6349.	11.29	11.51	11.72	11.83	11.84	11.77	11.82	17	7341.	10.89	11.10	11.29	11.37	11.35	11.29	11.35
	18	8306.	11.76	11.95	12.08	12.07	11.91	11.79	11.84									
9	0	−1307.	12.29	12.47	12.64	12.78	12.91	12.97	13.13	1	−1213.	11.34	11.53	11.71	11.84	11.97	12.03	12.17
	2	−1026.	11.62	11.82	12.00	12.13	12.25	12.30	12.44	3	−748.	11.04	11.25	11.45	11.57	11.67	11.70	11.82
	4	−383.	11.63	11.78	11.96	12.06	12.11	12.10	12.20	5	64.	11.77	11.81	11.78	11.72	11.65	11.59	11.66
	6	588.	12.51	12.40	12.23	12.14	12.07	12.00	12.07	7	1182.	12.33	12.35	12.19	11.91	11.63	11.50	11.54

Table 2 (continued)

v	j	ϵ_{vj}	10K	30K	100K	300K	1000K	3000K	10^4K	j	ϵ_{vj}	10K	30K	100K	300K	1000K	3000K	10^4K
	8	1839.	11.49	11.71	11.91	12.01	12.01	11.93	11.98	9	2551.	11.31	11.51	11.65	11.64	11.54	11.44	11.48
	10	3310.	11.45	11.68	11.90	12.02	12.00	11.90	11.94	11	4107.	10.92	11.14	11.35	11.47	11.48	11.41	11.45
	12	4932.	11.59	11.80	11.96	12.00	11.95	11.87	11.92	13	5776.	11.22	11.43	11.57	11.57	11.47	11.38	11.44
	14	6626.	11.27	11.50	11.72	11.86	11.88	11.84	11.90	15	7470.	10.89	11.11	11.31	11.42	11.44	11.38	11.43
	16	8294.	11.93	12.12	12.25	12.23	12.07	11.92	11.94									
10	0	1608.	12.89	13.11	13.29	13.34	13.30	13.21	13.24	1	1692.	11.88	12.09	12.28	12.36	12.34	12.25	12.29
	2	1859.	12.06	12.27	12.48	12.59	12.60	12.52	12.55	3	2106.	11.43	11.65	11.87	12.00	12.00	11.91	11.94
	4	2430.	12.47	12.63	12.70	12.60	12.42	12.30	12.32	5	2827.	11.33	11.54	11.74	11.83	11.81	11.73	11.77
	6	3289.	11.67	11.89	12.12	12.24	12.23	12.15	12.19	7	3810.	11.31	11.52	11.69	11.74	11.69	11.62	11.66
	8	4384.	11.52	11.74	11.96	12.09	12.10	12.04	12.10	9	5001.	11.16	11.37	11.56	11.62	11.59	11.52	11.58
	10	5653.	11.51	11.74	11.96	12.07	12.05	11.97	12.03	11	6329.	11.01	11.23	11.44	11.55	11.55	11.49	11.54
	12	7019.	12.30	12.42	12.42	12.28	12.11	11.99	12.03	13	7708.	10.99	11.21	11.43	11.57	11.61	11.54	11.57
	14	8383.	11.89	12.09	12.26	12.29	12.17	12.05	12.08									
11	0	4106.	12.76	12.98	13.19	13.31	13.32	13.27	13.33	1	4179.	11.79	12.01	12.23	12.35	12.37	12.32	12.38
	2	4323.	12.04	12.27	12.49	12.62	12.63	12.58	12.63	3	4537.	11.57	11.79	12.00	12.09	12.04	11.97	12.02
	4	4815.	12.26	12.45	12.57	12.55	12.44	12.35	12.39	5	5154.	11.34	11.56	11.76	11.86	11.86	11.80	11.84
	6	5547.	11.72	11.95	12.17	12.30	12.30	12.23	12.27	7	5986.	11.61	11.81	11.94	11.93	11.83	11.73	11.76
	8	6464.	11.66	11.88	12.10	12.23	12.24	12.18	12.21	9	6971.	12.55	12.47	12.26	12.03	11.82	11.70	11.72
	10	7495.	11.64	11.86	12.07	12.18	12.20	12.14	12.19	11	8025.	11.25	11.47	11.69	11.81	11.77	11.67	11.72
	12	8544.	11.82	12.04	12.23	12.31	12.26	12.17	12.22									
12	0	6141.	13.07	13.28	13.46	13.52	13.49	13.43	13.46	1	6201.	12.06	12.27	12.46	12.54	12.53	12.47	12.51
	2	6320.	12.24	12.46	12.66	12.77	12.78	12.73	12.78	3	6494.	11.56	11.78	12.00	12.13	12.16	12.11	12.16
	4	6720.	11.95	12.18	12.40	12.54	12.55	12.49	12.54	5	6991.	12.47	12.52	12.43	12.25	12.06	11.95	11.99
	6	7302.	12.00	12.21	12.39	12.46	12.43	12.37	12.42	7	7643.	11.32	11.54	11.76	11.89	11.92	11.86	11.91
	8	8004.	11.92	12.15	12.37	12.48	12.45	12.35	12.38	9	8373.	11.76	11.97	12.13	12.15	12.03	11.90	11.92
	10	8732.	11.95	12.17	12.38	12.50	12.49	12.42	12.45									
13	0	7649.	13.06	13.28	13.50	13.64	13.67	13.60	13.63	1	7694.	12.11	12.33	12.55	12.69	12.73	12.66	12.68
	2	7781.	12.37	12.60	12.82	12.97	13.00	12.93	12.95	3	7908.	11.81	12.03	12.26	12.40	12.42	12.33	12.36
	4	8069.	12.43	12.65	12.85	12.93	12.86	12.74	12.76	5	8258.	12.30	12.48	12.59	12.54	12.36	12.22	12.23
	6	8465.	12.39	12.60	12.78	12.84	12.76	12.66	12.69	7	8677.	11.74	11.96	12.17	12.28	12.26	12.19	12.23
14	0	8542.	13.62	13.83	14.03	14.11	14.05	13.95	13.97	1	8567.	12.66	12.88	13.08	13.16	13.11	13.02	13.04
	2	8614.	12.92	13.14	13.35	13.44	13.41	13.32	13.34	3	8678.	12.33	12.55	12.76	12.87	12.85	12.77	12.79

present $V^{(1)}$ results are close to the values of G, but one must remember that the $V^{(2)}$ values are closer to those of BW and, moreover, that the maximum of the cross-section $\sigma_{(v=0,j=0)\to d}$ obtained with $V^{(2)}$ is very close to the maximum of the normalized experimental cross-section by Schulz & Asundi (1967). Again, here, all results are within a factor of 2.

Finally, a comparison between the $v\to v'$ vibrational excitation cross-sections of BW and the present ones is given in Table 5a (electron energy = 6 eV) and b (electron energy = 8 eV). The present results are close to those of BW, which is a great improvement over previous work (see N). Also, one should note that there is very little difference between the $v\to v'$ cross-sections yielded by $V^{(1)}$ or $V^{(2)}$.

In conclusion, it appears that the $V^{(2)}$ potential allows for a considerable reduction of the inconsistencies pointed out by N and that the rate coefficients listed in Table 2 should be more reliable than previous ones, providing a better basis for astrophysical work.

5. Discussion and conclusion

The present work is an attempt to describe the inverse processes (1) and (2) in a more consistent way than was the case in previous work. Our choice of a potential combining the advantages of the functions recommended by BW for the short range, by SRDW for the middle range, and by BD for the long range, results in better agreements with the theoretical results of BW, as well as with the experiments on process (2) and on the thermal rate coefficient for process (1). However, the present branching ratios for process (1) differ from those of BD, which demonstrates that they are very sensitive to the quality of the internal potential. The experimental value of the thermal rate coefficient of SFF is much smaller, or smaller, than the theoretical values obtained with $V^{(1)}$ or $V^{(2)}$, respectively, which are within the experimental uncertainty of a factor of 2. On the other hand, the good agreement with the work by BW, G and Schulz & Asundi (1967) shows that the present $V^{(2)}$ potential is indeed an improvement.

Our work at least indicates that it is possible to reduce the inconsistencies pointed out by N by improving the complex potential description of processes (1) and (2). However, the validity of the local resonant scattering theory has yet to be fully defined. From an astrophysical point of view, the features of the IR emission spectrum of H_2 should be affected by the present changes in branching ratios. It is of course difficult to rate the accuracy of our results, as our study and the comparison with previous work shows how sensitive the cross-sections are to the

Table 3. Comparison between the DA cross-sections by BW and the present results obtained with the $V^{(1)}$ and $V^{(2)}$ potentials (see text). *a b* stands for $a \times 10^b$

v	j	E(eV)	σ_{DA}(cm^2)		
			BW	$V^{(1)}$	$V^{(2)}$
0	0	3.73	1.6 −21	3.0 −21	1.7 −21
0	1	3.73	1.7 −21	3.2 −21	1.8 −21
0	2	3.70	1.9 −21	3.5 −21	2.0 −21
0	3	3.65	2.3 −21	4.2 −21	2.4 −21
0	4	3.60	2.8 −21	5.2 −21	3.1 −21
0	5	3.53	3.7 −21	6.8 −21	4.7 −21
0	6	3.45	5.0 −21	9.3 −21	7.9 −21
0	7	3.35	7.2 −21	1.4 −20	1.3 −20
0	8	3.25	1.1 −20	2.0 −20	1.4 −20
0	10	3.13	2.2 −20	1.4 −20	1.4 −20
0	15	2.38	3.2 −19	7.8 −28	2.8 −22
0	20	1.63	5.5 −18	8.0 −38	1.9 −15
1	0	3.23	5.5 −20	8.8 −20	5.0 −20
2	0	2.73	8.0 −19	1.1 −18	6.3 −19
3	0	2.28	6.3 −18	7.9 −18	4.5 −18
4	0	1.85	3.2 −17	3.7 −17	2.1 −17
5	0	1.45	1.1 −16	1.2 −16	6.9 −17
6	0	1.08	3.0 −16	3.0 −16	1.7 −16
7	0	0.73	4.5 −16	4.4 −16	2.5 −16
8	0	0.40	3.5 −16	3.4 −16	1.9 −16
9	0	0.13	4.8 −16	4.6 −16	2.6 −16

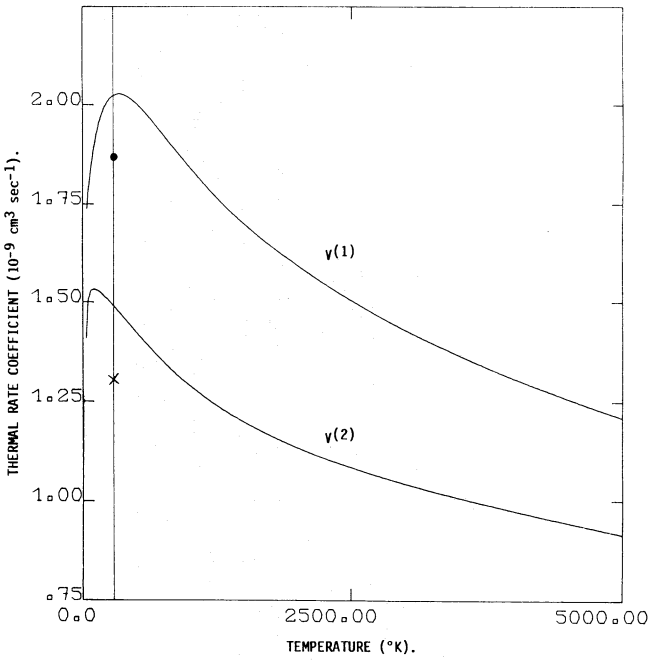

Fig. 3. Comparison between the present thermal rate coefficients obtained with potentials $V^{(1)}$ and $V^{(2)}$ (see text). The values calculated by BD (●) and measured by SFF (×) at 300 K are also displayed. The uncertainty on the experimental result is a factor of two

Table 4. Comparison between the maximum values (cm^2) for the DA cross-sections obtained by G and the present results yielded by the $V^{(1)}$ and $V^{(2)}$ potentials (see text). *a b* stands for $a \times 10^b$

v	j	G	$V^{(1)}$	$V^{(2)}$
0	0[c]	2.5 −21	3.0 −21	1.7 −21
0	5	7.0 −21	6.8 −21	4.7 −21
1	0	1.1 −19	8.8 −20	5.0 −20

[c] Absolute experimental measurement by Schulz & Asundi (1967): 1.6 −21

Table 5. Comparison between the results for vv' cross sections by BW and the present ones obtained with the $V^{(1)}$ or $V^{(2)}$ potentials (see text). *a b* stands for $a \times 10^b$

	$\sigma_{vv'}$ (Å^2)	
	BW	$V^{(1)}$ or $V^{(2)}$
(*a*) *Electron energy=6 eV*		
$v=0, v'=0$	9.5	8.6
1	2.6 −1	2.9 −1
2	2.0 −2	2.5 −2
3	2.4 −3	3.4 −3
4	3.9 −4	6.4 −4
5	8.3 −5	1.6 −4
(*b*) *Electron energy=8 eV*		
$v=0, v'=0$	5.9	5.1
1	1.7 −1	1.7 −1
2	1.1 −2	1.1 −2
3	1.2 −3	1.3 −3
4	2.3 −4	2.0 −4
5	6.9 −5	4.2 −5

details of the potential used. More work is obviously required before a firm opinion can be established in that respect.

In the future, we plan to investigate the $H+H^-$ problem using the *R*-matrix and Frame Transformation formalisms, in which the coupled motion of electrons and nuclei is treated rigorously (Le Dourneuf et al. 1983; Launay & Le Dourneuf 1984). In particular, we intend to build a more reliable potential by using a refined non-local function. This should provide a thorough check on the present results and those of BD or S.

Acknowledgements. The authors are grateful to Dr. J.P. Gauyacq for information on the potential by SRDW and to Prof. A. Dalgarno, Prof. A. Omont and Dr. E. Roueff for information on the astrophysical importance of the $H+H^-$ process. The calculations were performed at the CIRCE (Orsay, France) with time granted by the CNRS and at the CCVR (Ecole Polytechnique, Palaiseau, France) with time allocated by the Conseil Scientifique du Centre de Calcul Vectoriel pour la Recherche.

References

Allan M., Wong S.F., 1978, Phys. Rev. Lett. 41, 1791

Bardsley J.N., 1979, Invited Papers. Symposium on Electron-Molecule Collisions, eds. I. Shimamura, M. Matsuzawa, University of Tokyo, p. 121

Bardsley J.N., Wadehra J.M., 1979, Phys. Rev. A 20, 1398 (BW)

Bieniek R.J., 1980, J. Phys. B 13, 4405

Bieniek R.J., Dalgarno A., 1979, ApJ 228, 635 (BD)

Bishop D.M., Shih S.K., 1976, J. Chem. Phys. 64, 162

Black J.H., Porter A., Dalgarno A., 1981, ApJ 249, 138

Cederbaum L.S., Domcke W., 1981, J. Phys. B 14, 4665

Ehrhardt H., Langhans L., Linder F., Taylor H.S., 1968, Phys. Rev. 173, 222

Gauyacq J.P., 1985, J. Phys. B 18, 1859 (G)

Hall R.I., 1978, in: Physics of Electronic and Atomic Collisions. Invited Papers and Progress Reports X ICPEAC. North-Holland, Amsterdam, 25

Kolos W., Wolniewicz L., 1965, J. Chem. Phys. 43, 2429

Kolos W., Wolniewicz L., 1966, J. Chem. Phys. 45, 509

Kolos W., Wolniewicz L., 1968, J. Chem. Phys. 48, 3672

Launay J.M., Le Dourneuf M., 1984, in: Physics of Electronic and Atomic Collisions. Invited Papers and Progress Reports XIII ICPEAC, North Holland, Amsterdam, p. 635

Le Dourneuf M., Vo Ky L., Schneider B.I., 1983, in: Electron-Atom and Electron-Molecule Collisions, ed. J. Hinze, Plenum Press, New York and London, p. 135

Lepp S., Shull J.M., 1984, ApJ 280, 465

Nesbet R.K., 1981, Comments Atom. Molec. Phys. 11, 25 (N)

Palla F., Salpeter E.E., Stahler S.W., 1983, ApJ 271, 632

Rapp D., Sharp T.E., Briglia D.D., 1965, Phys. Rev. Lett. 14, 533

Sakimoto K., 1989, Chem. Phys. Lett. 164, 294 (S)

Schmeltekopf A.L., Fehsenfeld F.C., Ferguson E.E., 1967, ApJ 148, L155 (SFF)

Schulz G.J., 1959, Phys. Rev. 113, 816

Schulz G.J., Asundi R.K., 1967, Phys. Rev. 158, 25

Senekowitsch J., Rosmus P., Domcke W., Werner H.J., 1984, Chem. Phys. Lett. 111, 211 (SRDW)

Wadehra J.M., 1984, Phys. Rev. A 29, 106

Wadehra J.M., Bardsley J.N., 1978, Phys. Rev. Lett. 41, 1795